Talanta 115 (2013) 228–234

Contents lists available at ScienceDirect

Talanta

journal homepage: www.elsevier.com/locate/talanta

Direct electrochemistry of hemoglobin immobilized on the water-soluble phosphonate functionalized multi-walled carbon nanotubes and its application to nitric oxide biosensing

Pan Li [a], Yu Ding [a], Zhaoyang Lu [a], Ying Li [b], Xiaoshu Zhu [a,*], Yiming Zhou [a], Yawen Tang [a], Yu Chen [a,*], Chenxin Cai [a], Tianhong Lu [a]

[a] Jiangsu Key Laboratory of New Power Batteries, Center for Analysis and Testing, Laboratory of Electrochemistry, College of Chemistry and Materials Science, Nanjing Normal University, 1# Wenyuan Road, Nanjing 210023, PR China
[b] School of Chemistry and Chemical Engineering, Southeast University, Nanjing 210096, PR China

ARTICLE INFO

Article history:
Received 30 December 2012
Received in revised form
5 March 2013
Accepted 7 March 2013
Available online 6 May 2013

Keywords:
Phosphonic acid groups
Carbon nanotubes
Hemoglobin
Direct electrochemistry
Electrocatalysis

ABSTRACT

The direct electron transfer and electrocatalysis of hemoglobin (Hb) immobilized on the phosphonate functionalized multi-walled carbon nanotubes (MWCNTs) are investigated. Fourier transform infrared (FT-IR) spectra, UV–vis spectra and cyclic voltammetry (CV) analyses reveal that the phosphonate functionalized MWCNTs have good biocompatibility for Hb immobilization, and promote the electron communication between Hb and electrode. The immobilized Hb shows a pair of redox peak with a formal potential of -406 ± 10 mV (vs. SCE) and the electrochemical behavior of Hb was a surface-controlled process in a pH 7.0 phosphate buffer solution. And the immobilized Hb can act in an electrocatalytic manner in the electrochemical reduction of nitric oxide (NO). Accordingly, an unmediated NO electrochemical biosensor is constructed. Under optimized experimental conditions, the NO electrochemical biosensor shows the fast response (less than 3 s), the wide linear range (1.5×10^{-7} to 2.7×10^{-4} M) and the low detection limit (1.5×10^{-8} M), which is attributed to the good mass transport, the large Hb loading per unit area and the fast electron transfer rate of Hb.

© 2013 Elsevier B.V. All rights reserved.

1. Introduction

Nitric oxide (NO) is initially known as an environmental pollutant and toxin. However, recent investigations indicate the NO is an important bioregulator molecule involved in physiological functions such as blood pressure control, platelet aggregation, neurotransmission, immune surveillance, and vasodilation [1–3]. Consequently, the selective and sensitive detection of NO has received considerable attention. Among various proposed determination methods such as chemiluminescence, paramagnetic resonance, electrochemistry and spectrophotometry, the electrochemical determination of NO has received considerable interest due to simplicity, speed, sensitivity, and easy miniaturization of electrochemical instrumentation [4–6].

Since the end of 1970 s, the direct electron transfer (DET) of redox-active proteins has received considerable attention due to fundamental importance in life science and potential applications in the fabrication of biosensors, bioelectronics, biomedical devices, and bio-fuel cells [7–12]. Among various proteins and enzymes containing heme group, hemoglobin (Hb) is an ideal model molecule because of its known structure, commercial availability and relatively high stability [13–17]. But Hb can not undergo facile redox reaction at conventional electrode surface because their electroactive centers are embedded deeply in the protein shell, and the electrode passivation originated from protein adsorption restrains the DET between Hb and electrode [18].

To solve these problems, many modification methods have been developed, each with its own advantages and disadvantages. A relatively new method is to immobilize Hb on the various thiolates self-assembled monolayers (SAMs). In 2008, the biocompatible phosphonic acid ($-PO_3H_2$) terminated SAMs were used as a functional interface to immobilize Hb, and the DET of Hb was for the first time achieved on the well-defined electrochemically inactive SAMs [19]. Meanwhile, the immobilized Hb displayed the excellent bioelectrocatalytic activity towards the reduction of hydrogen peroxide [19]. Early studies contemplated that thiolates-SAMs were extraordinarily inert under ambient conditions [20]. However, the recent report indicated that the Au–S bond could be oxidized to sulfinate and/or sulfonate at ambient conditions [21]. In addition, the electrochemical reductive desorption and the electrochemical oxidation of thiolates-SAMs on the gold surface occurred at low potential and high potential, respectively [22].

* Corresponding authors. Tel.: +86 25 85891651; fax: +86 25 83243286.
E-mail address: ndchenyu@gmail.com (Y. Chen).

0039-9140/$ - see front matter © 2013 Elsevier B.V. All rights reserved.
http://dx.doi.org/10.1016/j.talanta.2013.03.088

Thus, the successful applications of thiolates-SAMs in electrochemical biosensors are extremely limited due to the instability of thiolates-SAMs and the narrow potential window of thiolates-SAMs modified gold electrode. For example, $–PO_3H_2$ terminated thiolates-SAMs modified gold electrode can not be used to construct the electrochemical biosensor for NO determination due to the electrochemical reductive desorption of thiolates-SAMs at low potential.

Since the discovery of carbon nanotubes (CNTs) in 1991, CNTs modified electrodes have been successfully utilized in the investigation of bioelectrochemical reaction and the preparation of biosensors due to their unique and interesting structural, mechanical and electronic properties [23–28]. However, the insolubility of CNTs in most solvents and their hydrophobicity limits their applications in the design of CNTs-based biosensing devices. Therefore, great efforts have been made to functionalize CNTs by covalent or noncovalent methods, aiming to improve their exfoliation and solubility in aqueous solution [23]. Compared with the covalent method, the noncovalent method can effectively preserve the electronic and structural integrity of pristine CNTs. Recent investigations indicated that ionic aromatic molecules had strong interactions with CNTs, such as π–π stacking interactions, charge–transfer interactions and hydrophobic effects in water, which could effectively solubilize CNTs and preserve the electronic and structural integrity of CNTs [29–31]. Our current work focus on the functionalized CNTs with the small aromatic molecules containing $–PO_3H_2$ groups because the $–PO_3H_2$ terminated interface can provide an ideal bio-mimic platform to immobilize proteins [19,32,33]. In addition, the small aromatic molecules modified CNTs may facilitate DET of immobilized proteins due to the short electron tunneling path of proteins and the high electron conductivity of aromatic molecules.

In the present work, the water-soluble phosphonate functionalized multi-walled carbon nanotubes (MWCNTs) are synthesized by π–π stacking interaction between naphthalen-1-ylmethylphosphonic acid (NYPA, shown in Scheme 1) and MWCNTs. Subsequently, the phosphonate functionalized MWCNTs successfully applied in studying the immobilization and DET of Hb for the first time. Experimental results demonstrate that the phosphonate functionalized MWCNTs can be a good candidate for protein immobilization and preparation of biosensors based on the direct electrochemistry of proteins without any electron transfer mediator.

2. Experimental

2.1. Reagents and chemicals

Hemoglobin (Hb, M=66000, from bovine blood) was provided by Sigma Co. Ltd. (USA) and used without further purification. Multi-walled carbon nanotubes (MWCNTs) (> 95% purity; surface area 138 $m^2 g^{-1}$) were purchased from Chengdu Organic Chemicals Co. Ltd., Chinese Academy of Sciences. Naphthalen-1-ylmethylphosphonic acid (NYPA, shown in Scheme 1) was gifted by Dr. Pengfei Wang at Nanjing University. The water-soluble phosphonate functionalized MWCNTs (i.e., NYPA-MWCNTs hybrids) were synthesized by the π–π stacking interaction between MWCNTs and NYPA. Briefly, 10 mg pristine MWCNTs was added into 10 mL of 5 mM NYPA aqueous solution (pH 9), then sonicated in ice water for 10 h. After filtration, the final products (i.e., NYPA-MWCNTs hybrids) were washed with Millipore water and then dried in a vacuum oven at 60 °C for 10 h to remove solvent. Saturated NO solution (1.9 mM) was prepared by dropping H_2SO_4 (6 M) into deoxygenated $NaNO_2$ saturated solution slowly [34,35], and then was used to prepare serial solutions of known NO concentration. All other reagents were of analytical grade and used without further purification. Phosphate buffer solutions (PBS, 0.1 M, pH=7.0) were prepared by mixing standard stock solutions of K_2HPO_4 and KH_2PO_4.

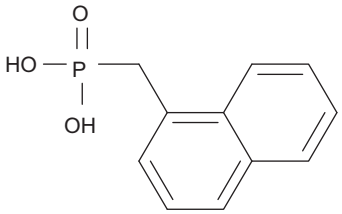

Scheme 1. Structure of naphthalen-1-ylmethylphosphonic acid (NYPA).

2.2. Preparation of the Nafion/Hb/NYPA-MWCNTs/GC electrode

One milligram NYPA-MWCNTs hybrids were well dispersed in 2 mL water (with the aid of ultrasonic agitation) to give a black suspension of 0.5 mg mL^{-1}. Fifty microliter of resultant NYPA-MWCNTs suspension was mixed well with 50 μL of Hb solution (3 mg mL^{-1}, pH 5) thoroughly. Then 4 μL of the mixture was dropped onto the glassy carbon (GC, CH Instruments, 3 mm diameter, 0.07 cm^2) electrode surface and allowed to dry at ambient temperature. Subsequently, the electrode was rinsed with Millipore water to remove the non-firmly adsorbed Hb and allowed to dry at ambient temperature, again. At last, 2.0 μL of 5 wt% Nafion solution was dropped onto the electrode surface to form a stable film, which could improve the adhering ability of NYPA-MWCNTs and Hb on the electrode surface [36]. The preparation process of modified electrode was shown in Scheme 2. The fabricated electrode was denoted as Nafion/Hb/NYPA-MWCNTs/GC and stored at 4 °C refrigerator when not in use. For comparison, the Nafion/Hb/GC and Nafion/MWCNTs/GC electrodes were also fabricated by the similar procedure.

2.3. Instruments

Surface area of MWCNTs was measured by nitrogen adsorption at 77 K on a Micromeritics ASAP 2020 instrument. X-ray photoelectron spectroscopy (XPS) measurements were carried out on a Thermo VG Scientific ESCALAB 250 spectrometer with an Mg Kα radiator. Scanning electron microscopy (SEM) images were obtained from a Hitachi S4800 scanning electron microscope. Fourier transform infrared (FT-IR) spectra were carried out using a Nicolet 520 SXFTIR spectrometer. The zeta potential analysis was performed with a Malvern Zetasizer Nano ZS90 analyzer at room temperature. The morphology of Hb immobilized MWCNTs surface was monitored on an Agilent Series 5100 atomic force microscope (AFM) in tapping mode. UV–vis spectra were recorded at room temperature on a UV3600 spectrophotometer. Circular dichroism (CD) spectra were recorded with a Chirascan circular dichroism spectrometer (Applied Photphysics).

Electrochemical measurements were performed using a CHI 660C electrochemical analyzer in a conventional three-electrode electrochemical cell. A Pt plate auxiliary electrode and a saturated calomel reference electrode (SCE) were used. All potentials in this study were reported with respect to SCE. Prior to the electrochemical measurements, N_2 was bubbled through the solution for 10 min to remove the dissolved O_2. All the electrochemical measurements were carried out at 25 ± 1 °C.

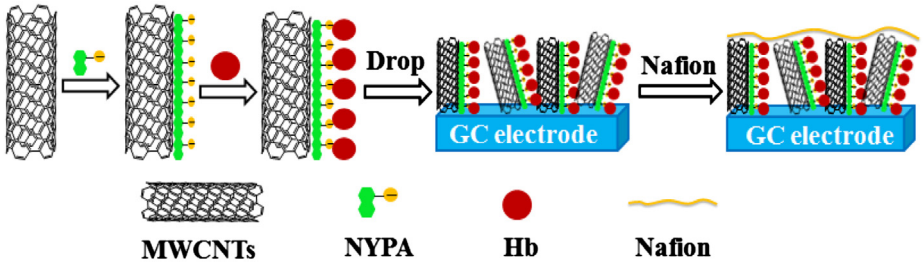

Scheme 2. Illustration of the preparation process of Nafion/Hb/NYPA-MWCNTs/GC electrode.

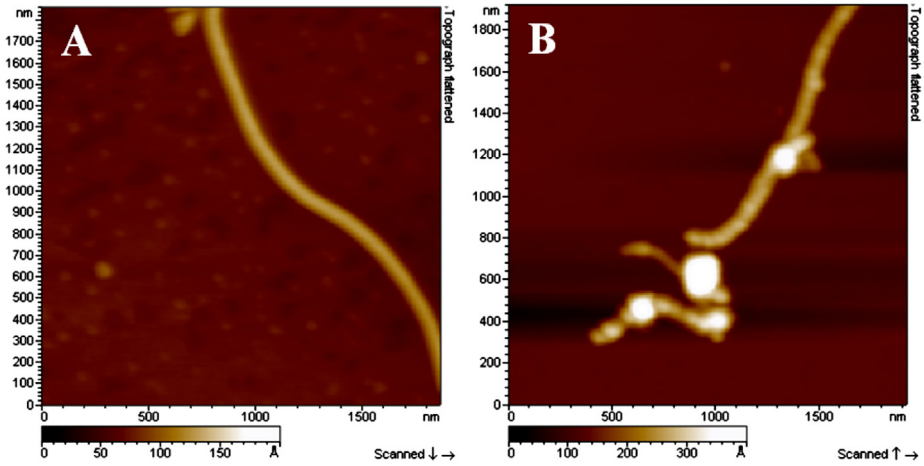

Fig. 1. AFM images of (A) NYPA-MWCNTs hybrids and (B) Hb/NYPA-MWCNTs sample.

3. Results and discussion

3.1. Characterization of NYPA-MWCNTs hybrids

It is known that the biosensor applications of pristine MWCNTs are extremely limited due to the insolubility in aqueous solution (Fig. S1A) and incompatibility with most biological systems [37,38], which originate from their inert graphitic nature, strong hydrophobicity and strong intertube van der Waals interactions. After sonicating the mixture solution of MWCNTs and NYPA (pH 9) for 10 h, an evenly distributed black suspension is obtained, as shown in Fig. S1B. The black homogeneous dispersion can be essentially stable for at least 3 months, indicating that NYPA molecules have been successfully immobilized on MWCNTs surface via a π–π stacking interaction. The zeta potential of NYPA-MWCNTs hybrids is -45 ± 5 mV at pH 9, suggesting the naphthyl groups of NYPA are attached to the MWCNTs surface while phosphonate groups remain free on the chain end. For comparison, the zeta potential of carboxylated MWCNTs is only -23 ± 6 mV under the same pH conditions. Since $-PO_3H_2$ group is a dibasic acid, the electrostatic repulsion between $-PO_3^{2-}$ species is expected to be much stronger than that between COO^- groups according to Coulomb's law. Thus, the zeta potential of NYPA-MWCNTs hybrids is more negative than that of carboxylated MWCNTs. Consequently, the strong electrostatic repulsion between phosphonate groups is responsible for the excellent colloidal stability of NYPA-MWCNTs hybrids.

3.2. Interaction between Hb and NYPA-MWCNTs hybrids

XPS was used to verify Hb adsorption on NYPA-MWCNTs hybrids (Fig. S2). The N 1 s signal is assigned to the amide linkages and to nitrogen-containing side chains such as lysine and histidine. Therefore, the appearance of the N 1 s peak (400.4 eV) confirms that the Hb have adsorbed on the surface of NYPA-MWCNTs hybrids. The adsorption of Hb on the surface of NYPA-MWCNTs hybrids was also imaged by AFM. Fig. 1 shows AFM images of NYPA-MWCNTs hybrids and Hb/NYPA-MWCNTs sample. Comparing the two images, it is directly observed that some Hb adsorb on the surface of NYPA-MWCNTs hybrids.

SEM is a powerful tool for studying the surface morphology of film. Fig. 2 shows SEM images of NYPA-MWCNTs hybrids and Hb/NYPA-MWCNTs sample on GC electrode. As observed, the NYPA-MWCNTs hybrids film shows a network-like structure (Fig. 2A). This feature is attractive for the further development of electrochemical biosensors because such a three-dimensional configuration can essentially increase the loading of enzymes/proteins [39] and restrict the loss of immobilized enzymes/proteins [5,33]. For Hb/NYPA-MWCNTs sample, SEM image shows the three-dimensional network-like structure still retains constant (Fig. 2B), which facilitates mass transport of analytes, and consequently increases the sensitivity of electrochemical response [23,33,40,41].

Since the isoelectric point of bovine Hb protein is about 6.9 [42], Hb are positively charged in a pH 5.0 solution. In contrast, NYPA-MWCNTs hybrids are negatively charged in a pH 5.0 solution because the zeta potential of NYPA-MWCNTs hybrids is -27 ± 5 mV in a pH 5.0 solution. Thus, the electrostatic interaction between the positively charged Hb and the negatively charged NYPA-MWCNTs hybrids may result in the immobilization of Hb on NYPA-MWCNTs hybrids. It is clear that proteins have many $-NH_2$ groups in their polypeptide backbones. Considering the strong hydrogen-bonding interaction between $-PO_3H_2$ and $-NH_2$ groups [43–46], we presume that the interaction between NYPA and Hb may also involve in the hydrogen-bonding interaction between $-PO_3H_2$ groups in NYPA and $-NH_2$ groups in the polypeptide backbones of Hb, which is also responsible for immobilization of Hb on NYPA-MWCNTs hybrids.

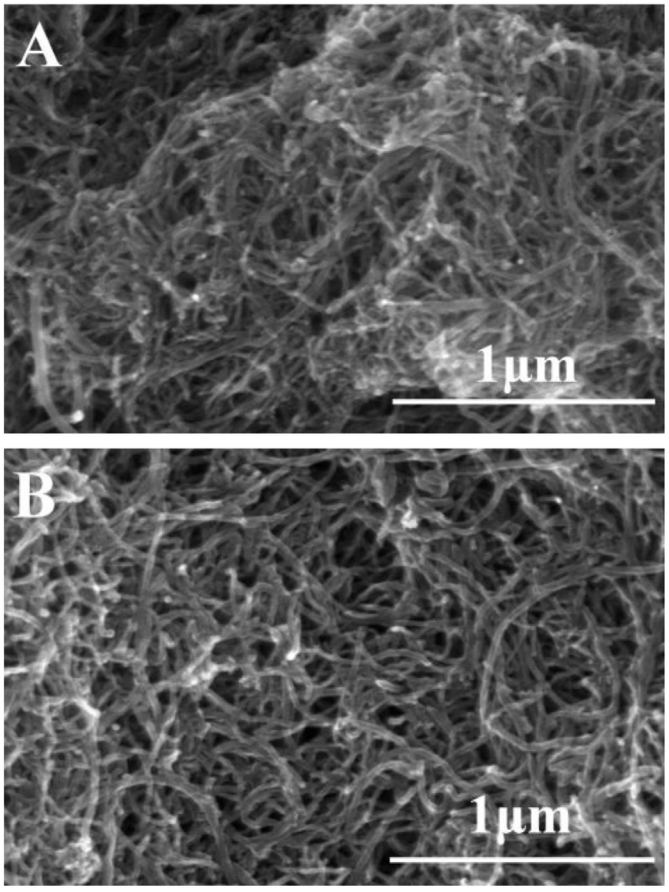

Fig. 2. SEM images of (A) NYPA-MWCNTs hybrids and (B) Hb/NYPA-MWCNTs sample.

The positions of the amide bands can provide information about secondary structure of polypeptide chain because their positions are sensitive to protein peptide chain conformational change [47]. The amide I band (1700–1600 cm^{-1}) and the amide II band (1600–1500 cm^{-1}) are ascribed to the C=O stretching vibration of peptide linkages in the backbone of Hb and a combination of N–H bending and C–N stretching in Hb, respectively [47]. As observed, the shape and position of these two bands for Hb immobilized on NYPA-MWCNTs hybrids are similar to those of native Hb (Fig. 3A), that is, the adsorbed Hb retains their native structure. The secondary structure of Hb immobilized on NYPA-MWCNTs hybrids was further investigated by CD spectra (Fig. 3B). The CD spectrum of native Hb exhibits two negative bands at 208 and 222 nm (Fig. 3B, curve a), which is a characteristic of an α-helix structure of protein [48]. The band at 208 nm corresponds to π–π^* transition of the α-helix, whereas the band at 222 nm corresponds to π–π^* transition for both the α-helix and random coil. After addition of NYPA-MWCNTs hybrids, there are no remarkable variations occurring in the shape and position of the characteristic ellipticity bands for Hb (Fig. 3B, curve b), indicating that the structural organizations of the polypeptide chain in Hb still preserve. UV–vis spectroscopy is a useful tool for the conformational study of heme proteins. The Soret absorption band of the heme prosthetic group can provide information on the tertiary structure of heme proteins, especially the conformational change around the heme region [47,49–51]. It is clear that no characteristic absorption of NYPA-MWCNTs hybrid is observed in the UV–vis spectrum (Fig. 3C, curve a). For comparison, dry Hb/NYPA-MWCNTs hybrids films display a maximum absorption at 405 nm (Fig. 3C, curve b), as almost the same as that of the native Hb (Fig. 3C, curve c). The similarity of the two spectra indicates that Hb immobilized on NYPA-MWCNTs hybrids retains their near-native conformation [47,49–51]. Thus, FT-IR, CD and UV–vis measurements indicate that NYPA-MWCNTs hybrids may provide

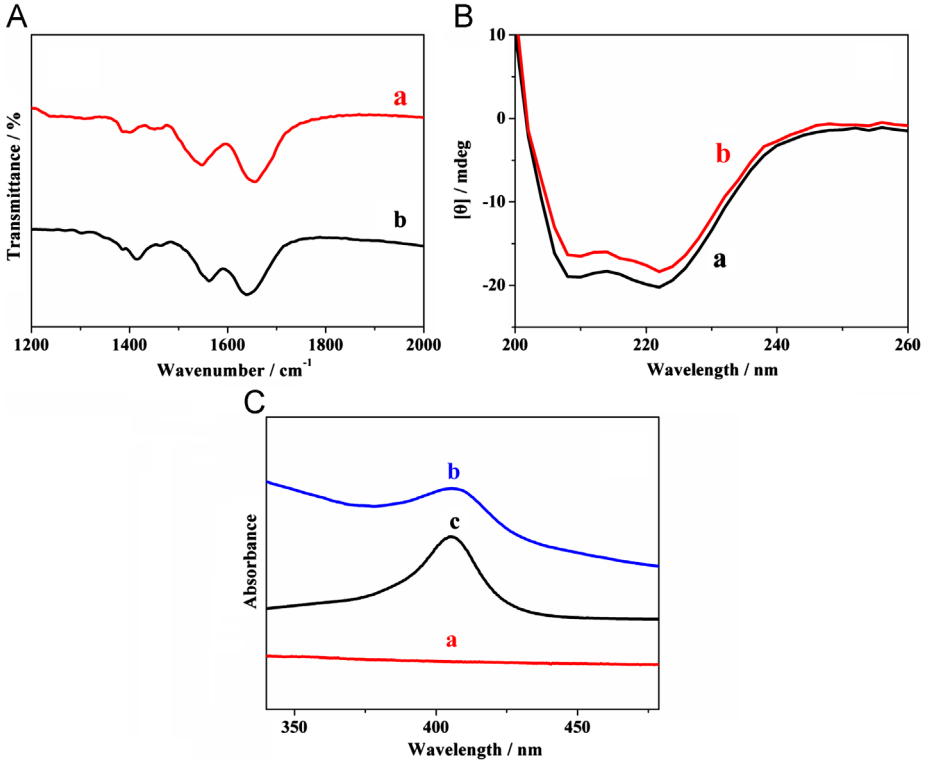

Fig. 3. (A) FT-IR spectra of (a) native Hb and (b) dry Hb/NYPA-MWCNTs hybrids film. (B) CD spectra of (a) native Hb and (b) Hb/NYPA-MWCNTs hybrids. (C) UV–vis spectra of (a) NYPA-MWCNTs hybrid, (b) dry Hb/NYPA-MWCNTs hybrid film and (c) native Hb solution.

a promising matrix for the proteins immobilization and the biosensor fabrication because of their satisfying biocompatibility.

3.3. Direct electrochemistry of Hb

Fig. 4 depicts typical cyclic voltammograms of Nafion/GC, Nafion/NYPA-MWCNTs/GC and Nafion/Hb/NYPA-MWCNTs/GC electrodes in pH 7.0 PBS. As shown, no redox peaks are observed at Nafion/GC and Nafion/NYPA-MWCNTs/GC electrode in the potential range of interest (Fig. 4a and b), indicating that no electroactive species exist on the surface of Nafion/GC and Nafion/NYPA-MWCNTs/GC electrodes. However, a pair of well defined and nearly symmetric redox peaks is obtained at the Nafion/Hb/NYPA-MWCNTs/GC electrode (Fig. 4c), attributable to the characteristics of the Fe^{III}/Fe^{II} redox couple of the immobilized Hb. The formal potential ($E^{\circ\prime}$, defined as the average of the anodic peak potential, E_{pa} and the cathodic potential, E_{pc}) is about -406 ± 10 mV. The separation of the peak potential (ΔEp) is 36 ± 8 mV. With the increase of scan rate, the $E^{\circ\prime}$ of the Nafion/Hb/NYPA-MWCNTs/GC electrode is almost unchanged, while the anodic and cathodic peak currents increase linearly with the scan rate (Fig. S3A and B), showing a surface-controlled electrode process. The above experiments present strong evidence that the phosphonate functionalized MWCNTs can provide a suitable biocompatible microenvironment to immobilize Hb and facilitate the direct electron transfer of Hb.

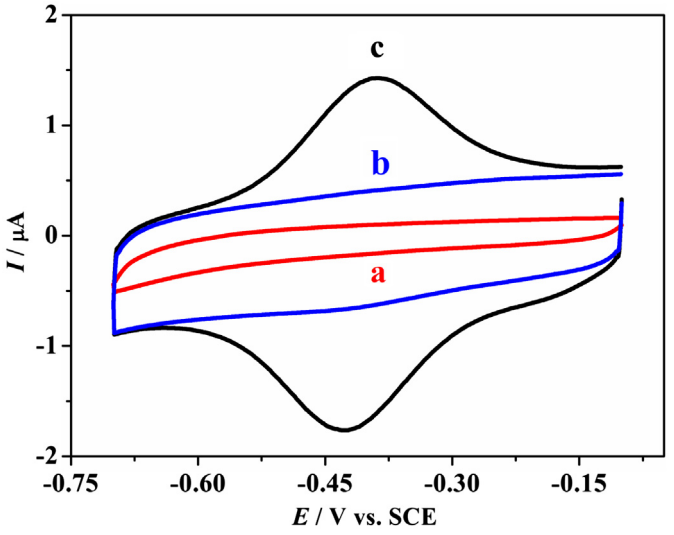

Fig. 4. Cyclic voltammograms of (a) Nafion/GC, (b) Nafion/NYPA-MWCNTs/GC and (c) Nafion/Hb/NYPA-MWCNTs/GC electrodes in 0.1 M PBS at a scan rate of 50 mV s^{-1}.

For a thin-layer electrochemistry, the surface coverage of electroactive species on electrode could be calculated by applying the Faradic equation [19,52]. In the present case, the calculated surface coverage for the electroactive Hb is 5.11×10^{-10} mol cm^{-2} (NOTING: the geometric area of the GC electrode is used in the Faradic equation because the effective electrode surface of MWCNTs modified GC electrode can not be measured electrochemically by probe molecules, owing to the unknown diffusion equation), which is 27 times larger than the theoretically compacted monolayer coverage of Hb (1.89×10^{-11} mol cm^{-2}) [19,53,54]. BET measurement shows that MWCNTs have a large specific surface area (180.6 m^2 g^{-1}). Thus, the introduction of MWCNTs on GC electrode increases the effective electrode surface area for Hb immobilization, and consequently results in an increase in the active sites of Hb on the electrode surface [55]. The charge–transfer rate constant (k_s) of the Hb at the Nafion/Hb/NYPA-MWCNTs/GC electrode is estimated to be 12.69 s^{-1} at a scan rate of 1 V s^{-1} based on the Laviron equation [56]. This value is much larger than the ones reported for the Hb immobilized on the various functionalized MWCNTs modified electrode (form 0.7 to 9.5 s^{-1}, Table S1), which is likely attributed to the excellent biocompatibility of NYPA-MWCNTs hybrids, the short electron

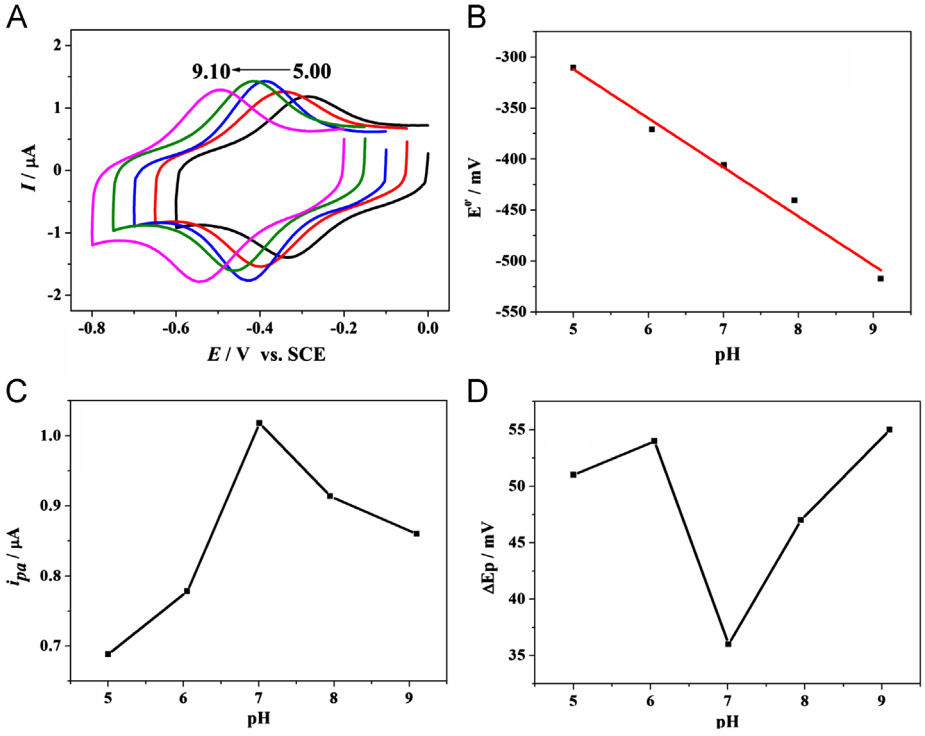

Fig. 5. (A) Cyclic voltammograms of the Nafion/Hb/NYPA-MWCNTs/GC electrode in a 0.1 M PBS at different pH value of 5.00, 6.05, 7.01, 7.95 and 9.10 (from right to left) at a scan rate of 50 mVs^{-1}. (B) Effect of pH on the formal potential (E0′). (C) Effect of pH on the ipa. (D) Effect of pH on the ΔEp.

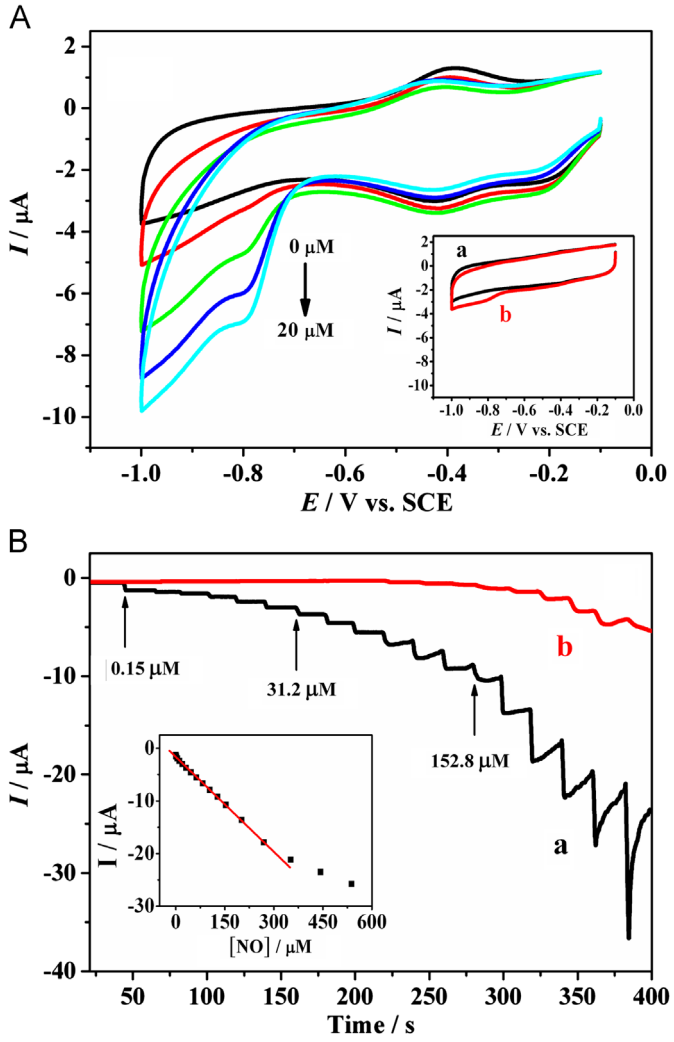

Fig. 6. (A) Cyclic voltammograms of Nafion/Hb/NYPA-MWCNTs/GC electrode in PBS (pH 7.0) containing (a) 0, (b) 0.9, (c) 6, (d) 13 and (e) 20 μM NO at a scan rate of 50 mVs^{-1}. Inset: Cyclic voltammograms of Nafion/NYPA-MWCNTs/GC electrode in PBS (pH 7.0) containing (a) 0 and (b) 20 μM NO at a scan rate of 50 mVs^{-1}. (B) Dynamic responses of (a) Nafion/Hb/NYPA-MWCNTs/GC and (b) Nafion/NYPA-MWCNTs/GC electrodes to successive addition of 1.9 mM NO in the solution at the applied potential of −0.85 V under continuous stirring condition. Inset: calibration plot between current and NO concentration.

tunneling transfer path of Hb (i.e., the small molecule size of immobilized NYPA molecules), and the high electron conductivity of aromatic molecule [57–59].

It is known that solution pH modulates the protonation of distal and/or proximal histidines, or the protonation of the water molecule coordinated to the central iron, and accordingly influences the redox potential of Hb [47,60,61]. Thus, the dependence of the electrochemical behavior of Nafion/Hb/NYPA-MWCNTs/GC electrode on solution pH is investigated (Fig. 5A). It is observed that the $E^{\circ\prime}$ decreases linearly with the solution pH with a slope of -48.1 ± 5 mV per decade pH in the whole pH range of 5.00–9.10 (Fig. 5B), which is reasonably close to the theoretical value of −58 mV pH^{-1} for a reversible one-electron coupled one-proton reaction process at 25 °C. Moreover, it is clear that solution pH affects the redox current of Nafion/Hb/NYPA-MWCNTs/GC electrode (Fig. 5C). At pH value lower than the isoelectric point (p*I*=6.9) of Hb [42], the peak current increases with increasing pH, and it reaches the maximum as the solution pH is closing to the p*I* of Hb. With further increase of solution pH, the peak current decreases. Meanwhile, the dependence of Δ*E*p value on solution pH also shows a similar change tendency (Fig. 5D). For example, Δ*E*p of electrode reaches the minimum as solution pH is closing to the p*I* of Hb. Till now, all electrochemical parameters indicate that the electron transfer rate of Nafion/Hb/NYPA-MWCNTs/GC electrode reaches the maximum at ca. pH 7.0. Thus, a pH value of 7.0 is chosen as the optimum and used in further experiments.

3.4. Electrocatalytic activity of Nafion/Hb/NYPA-MWCNTs/GC electrode for the reduction of nitric oxide

Fig. 6A shows the cyclic voltammograms of Nafion/Hb/NYPA-MWCNTs/GC electrode in PBS (pH 7.0) containing different NO concentrations. A pair of reversible redox peaks at approximately −0.41 V is assigned to the Fe^{III}/Fe^{II} couples in Hb. On addition of NO solution to PBS, a new cathodic peak appears at about −0.78 V, which is assigned to the reduction peak of NO [61,62]. Meanwhile, the reduction peak currents increase with NO concentrations, indicating that the modified electrode can be used as a biosensor to quantificationally detect the concentration of NO. In controlled experiment, the direct reduction of NO at Nafion/NYPA-MWCNTs/GC electrode is hardly observed in the studied potential window (inset in Fig. 6A), suggesting that the bioelectrocatalytic activity of the Nafion/Hb/NYPA-MWCNTs/GC electrode towards reduction of NO is attributed to the electroactive center of Hb. Based on the literature [5], the mechanism for the electrocatalytic reduction of NO may be expressed as the following schemes:

$$HbFe(III)+e+H^+ \rightarrow HbFe(II) \quad (1)$$

$$HbFe(II)+NO \rightarrow HbFe(II)–NO \quad (2)$$

$$2HbFe(II)–NO+2e+2H^+ \rightarrow 2HbFe(II)+H_2O+N_2O \quad (3)$$

In addition, the amperometric response of the Nafion/Hb/NYPA-MWCNTs/GC electrode is significant and very quick upon addition of NO solution (Fig. 6B, curve a). The electrochemical response of this sensor reaches 95% of the steady-state current in less than 3 s. Such a speedy response may be attributed to the three-dimensional network structure of Nafion/Hb/NYPA-MWCNTs/GC electrode with unlimited mass diffusion. On the other hand, the response of NO on the Nafion/NYPA-MWCNTs/GC electrode is negligible (Fig. 6B, curve b), further indicating that the observed amperometric responses on the Nafion/Hb/NYPA-MWCNTs/GC electrode are due to the immobilized Hb. The inset in Fig. 6B displays the calibration plot of the sensor. The current response shows a linear relationship with the concentration of NO ranging from 1.5×10^{-7} to 2.7×10^{-4} M with a correlation coefficient of 0.9987. The detection limit is 1.5×10^{-8} M at a signal-to-noise ratio of 3. The performance of the present biosensor is better than other NO electrochemical sensors (Table S2), which is attributed to the good mass transport, larger Hb loading per unit area and fast electron transfer rate of the immobilized Hb. Meanwhile, it is observed that the detection limit or linear range of present biosensor for the determination of NO is comparable to that of no-electrochemical methods such as fluorescent [63,64], spectrophotometric [65] and colorimetric methods [66,67], confirming the high sensitivity of the present NO biosensor. Furthermore, the Nafion/Hb/NYPA-MWCNTs/GC electrode also shows an excellent electrocatalytic performance towards the reduction of H_2O_2 (Fig. S4A). The resultant H_2O_2 electrochemical biosensor shows the fast response (less than 3 s), the wide linear range (4.0×10^{-6} to 1.2×10^{-3} M) with a correlation coefficient of 0.996, and the low detection limit (4.0×10^{-7} M) at a signal-to-noise ratio of 3 (Fig. S4B).

The reproducibility of the sensor was also examined electrochemically in a solution containing 0.1 mM NO with the same sensor, and the relative standard deviation was 4.3% (n=9).

After measurement, the sensor was rinsed with Millipore water and stored at 4 °C, and it was found that the sensor retained its activity about 91% of its initial value after 10 days and about 80% after 30 days. The excellent long-term stability could be attributed to the biocompatibility of NYPA-MWCNTs hybrids film.

4. Conclusions

The water-soluble phosphonate functionalized MWCNTs can provide an ideal bio-mimic platform to immobilize Hb owing to their excellent biocompatibility. Compared with the other various functionalized MWCNTs, the present NYPA-MWCNTs hybrids facilitate the direct electron transfer between Hb and electrode due to the short electron tunneling transfer path of Hb (i.e., the small molecule size of NYPA) and the high electron conductivity of aromatic molecule. Compared with the biocompatible $–PO_3H_2$ terminated thiolate-SAMs, the phosphonate functionalized MWCNTs modified electrode shows the better chemical stability and the wider potential window, which may extend the potential applications of the $–PO_3H_2$ terminated functional interface in the field of electrochemical biosensors. Consequently, the Nafion/Hb/NYPA-MWCNTs/GC electrode can be used as an electrochemical biosensor to catalyze the reduction of nitric oxide.

Acknowledgments

The authors are grateful for the financial support of National Natural Science Foundation of China (21005039) and a Project Funded by the Priority Academic Program Development of Jiangsu Higher Education Institutions.

Appendix A. Supporting information

Supplementary data associated with this article can be found in the online version at http://dx.doi.org/10.1016/j.talanta.2013.03.088.

References

[1] S. Moncada, R. Palmer, E. Higgs, Pharmacol. Rev. 43 (1991) 109–142.
[2] N. Toda, T. Okamura, Pharmacol. Rev. 55 (2003) 271–324.
[3] K.M. Miranda, Coordin. Chem. Rev. 249 (2005) 433–455.
[4] S. Jia, J. Fei, J. Zhou, X. Chen, J. Meng, Biosens. Bioelectron. 24 (2009) 3049–3054.
[5] Y.J. Li, C. Liu, M.H. Yang, Y. He, E.S. Yeung, J. Electroanal. Chem. 622 (2008) 103–108.
[6] R. Trouillon, Biol. Chem. 394 (2013) 17–33.
[7] I. Platzman, H. Haick, R. Tannenbaum, ACS Appl. Mater. Interface 2 (2010) 2585–2593.
[8] S. Chaterji, I.K. Kwon, K. Park, Prog. Polym. Sci. 32 (2007) 1083–1122.
[9] Y. Zhang, J. Zhang, H. Wu, S. Guo, J. Zhang, J. Electroanal. Chem. 681 (2012) 49–55.
[10] E. Repo, E. Ahlberg, L. Murtomaki, K. Kontturi, D.J. Schiffrin, Electrochim. Acta 54 (2009) 6584–6593.
[11] B. Viguier, K. Zor, E. Kasotakis, A. Mitraki, C. Hyttel Clausen, W.E. Svendsen, J. Castillo-Leon, ACS Appl. Mater. Interface 3 (2011) 1594–1600.
[12] A.K.M. Kafi, G. Wu, P. Benvenuto, A. Chen, J. Electroanal. Chem. 662 (2011) 64–69.
[13] H. Zhang, L. Fan, S. Yang, Chem-Eur. J. 12 (2006) 7161–7166.
[14] Y. Liu, C. Lu, W. Hou, J.J. Zhu, Anal. Biochem. 375 (2008) 27–34.
[15] S.W. Tan, X.C. Tan, J.Y. Jiang, J. Xu, J.L. Zhang, D.D. Zhao, L. Liu, Z.Y. Huang, J. Electroanal. Chem. 668 (2012) 113–118.
[16] S. Garabagiu, G. Mihailescu, J. Electroanal. Chem. 659 (2011) 196–200.
[17] D. Nie, Y. Liang, T. Zhou, X. Li, G. Shi, L. Jin, Bioelectrochemistry 79 (2010) 248–253.
[18] G. Shi, Z. Sun, M. Liu, L. Zhang, Y. Liu, Y. Qu, L. Jin, Anal. Chem. 79 (2007) 3581–3588.
[19] Y. Chen, B. Jin, L.R. Guo, X.J. Yang, W. Chen, G. Gu, L.M. Zheng, X.H. Xia, Chem-Eur. J. 14 (2008) 10727–10734.
[20] P.E. Laibinis, G.M. Whitesides, J. Am. Chem. Soc. 114 (1992) 9022–9028.
[21] C. Zhou, A.V. Walker, Langmuir 22 (2006) 11420–11425.
[22] Y. Chen, C. Yang, F.B. Wang, Electrochim. Acta 55 (2010) 3951–3956.
[23] P. Li, H. Liu, Y. Ding, Y. Wang, Y. Chen, Y. Zhou, Y. Tang, H. Wei, C. Cai, T. Lu, J. Mater. Chem. 22 (2012) 15370–15378.
[24] Y. Zeng, D. Yu, Y. Yu, T. Zhou, G. Shi, J. Hazard. Mater. 217–218 (2012) 315–322.
[25] D. Zhang, D. Yu, W. Zhao, Q. Yang, H. Kajiura, Y. Li, T. Zhou, G. Shi, Analyst 137 (2012) 2629–2636.
[26] S. Liu, B. Lin, X. Yang, Q. Zhang, J. Phys. Chem. B 111 (2007) 1182–1188.
[27] X. Xu, S. Jiang, Z. Hu, S. Liu, ACS Nano 4 (2010) 4292–4298.
[28] X. Xu, L. Yang, S. Jiang, Z. Hu, S. Liu, Chem. Commun. 47 (2011) 7137–7139.
[29] Y.K. Kang, O.S. Lee, P. Deria, S.H. Kim, T.H. Park, D.A. Bonnell, J.G. Saven, M. J. Therien, Nano Lett. 9 (2009) 1414–1418.
[30] F.Y. Cheng, A. Adronov, Chem-Eur. J. 12 (2006) 5053–5059.
[31] M. Fagnoni, A. Profumo, D. Merli, D. Dondi, P. Mustarelli, E. Quartarone, Adv. Mater. 21 (2009) 1761–1765.
[32] Y. Chen, X.J. Yang, L.R. Guo, B. Jin, X.H. Xia, L.M. Zheng, Talanta 78 (2009) 248–252.
[33] Y. Chen, X.J. Yang, L.R. Guo, J. Li, X.H. Xia, L.M. Zheng, Anal. Chim. Acta 644 (2009) 83–89.
[34] S. Trevin, F. Bedioui, J. Devynck, J. Electroanal. Chem. 408 (1996) 261–265.
[35] G.C. Zhao, L. Zhang, X.W. Wei, Z.S. Yang, Electrochem. Commun. 5 (2003) 825–829.
[36] Y. Zhang, J.B. Zheng, Chin. J. Chem. 29 (2011) 685–690.
[37] C.W. Doe, S.M. Choi, S.R. Kline, H.S. Jang, T.H. Kim, Adv. Funct. Mater. 18 (2008) 2685–2691.
[38] Q. Yang, X.J. Pan, Ind. Eng. Chem. Res. 49 (2010) 2747–2751.
[39] W. Zheng, Y.Q. Chen, Y.F. Zheng, Appl. Surf. Sci. 255 (2008) 571–573.
[40] M. Zheng, Y. Zhou, Y. Chen, Y. Tang, T. Lu, Electrochim. Acta 55 (2010) 4789–4798.
[41] C. Wang, C. Yang, Y. Song, W. Gao, X. Xia, Adv. Funct. Mater. 15 (2005) 1267–1275.
[42] Z.O. Araci, A.F. Runge, W.J. Doherty III, S.S. Saavedra, J. Am. Chem. Soc. 130 (2008) 1572–1573.
[43] A. Ojida, M. Inoue, Y. Mito-oka, H. Tsutsumi, K. Sada, I. Hamachi, J. Am. Chem. Soc. 128 (2006) 2052–2058.
[44] L.N. Johnson, R.J. Lewis, Chem. Rev. 101 (2001) 2209–2242.
[45] S. Anderson, U. Neidlein, V. Gramlich, F. Diederich, Angew. Chem. Int. Ed. 34 (1995) 1596–1600.
[46] A.A. Gorfe, M. Hanzal-Bayer, D. Abankwa, J.F. Hancock, J.A. McCammon, J. Med. Chem. 50 (2007) 674–684.
[47] H.Y. Zhao, W. Zheng, Z.X. Meng, H.M. Zhou, X.X. Xu, Z. Li, Y.F. Zheng, Biosens. Bioelectron. 24 (2009) 2352–2357.
[48] Q. Shao, P. Wu, P. Gu, X. Xu, H. Zhang, C. Cai, J. Phys. Chem. B 115 (2011) 8627–8637.
[49] W. Sun, X.Q. Li, Y. Wang, X. Li, C.Z. Zhao, K. Jiao, Bioelectrochemistry 75 (2009) 170–175.
[50] Y.L. Wen, H.X. Wu, S.H. Chen, Y.H. Lu, H.B. Shen, N.Q. Jia, Electrochim. Acta 54 (2009) 7078–7084.
[51] W. Zheng, Y.F. Zheng, Electrochem. Commun. 9 (2007) 1619–1623.
[52] M. Zheng, P. Li, C. Yang, H. Zhu, Y. Chen, Y. Tang, Y. Zhou, T. Lu, Analyst 137 (2012) 1182–1189.
[53] Q. Lu, C. Hu, R. Cui, S. Hu, J. Phys. Chem. B 111 (2007) 9808–9813.
[54] Y. Chen, F.B. Wang, L.R. Guo, L.M. Zheng, X.H. Xia, J. Phys. Chem. C 113 (2009) 3746–3750.
[55] W. Cao, C.M. Wei, J.B. Hu, Q.L. Li, Electroanalysis 20 (2008) 1925–1931.
[56] E. Laviron, J. Electroanal. Chem. 101 (1979) 19–28.
[57] A. Honciuc, R.M. Metzger, A. Gong, C.W. Spangler, J. Am. Chem. Soc. 129 (2007) 8310–8319.
[58] P. Si, Q. Chi, Z. Li, J. Ulstrup, P.J. Moller, J. Mortensen, J. Am. Chem. Soc. 129 (2007) 3888–3896.
[59] A. Dube, A.R. Chadeayne, M. Sharma, P.T. Wolczanski, J.R. Engstrom, J. Am. Chem. Soc. 127 (2005) 14299–14309.
[60] C. Lei, U. Wollenberger, N. Bistolas, A. Guiseppi-Elie, F.W. Scheller, Anal. Bioanal. Chem. 372 (2002) 235–239.
[61] L. Chen, G.X. Lu, J. Electroanal. Chem. 597 (2006) 51–59.
[62] L. Zhang, G.C. Zhao, X.W. Wei, Z.S. Yang, Electroanalysis 17 (2005) 630–634.
[63] M.H. Lim, B.A. Wong, W.H. Pitcock Jr, D. Mokshagundam, M.-H. Baik, S. J. Lippard, J. Am. Chem. Soc. 128 (2006) 14364–14373.
[64] M.H. Lim, S.J. Lippard, Inorg. Chem. 45 (2006) 8980–8989.
[65] L.A. Ridnour, J.E. Sim, M.A. Hayward, D.A. Wink, S.M. Martin, G.R. Buettner, D. R. Spitz, Anal. Biochem. 281 (2000) 223–229.
[66] R.W. Nims, J.C. Cook, M.C. Krishna, D. Christodoulou, C. Poore, A.M. Miles, M. B. Grisham, D.A. Wink, Methods Enzymol. 268 (1996) 93–105.
[67] R.W. Nims, J.F. Darbyshire, J.E. Saavedra, D. Christodoulou, I. Hanbauer, G. W. Cox, M.B. Grisham, F. Laval, J.A. Cook, M.C. Krishna, Methods 7 (1995) 48–54.